



DEFORMATION AND FRACTURE OF PST CRYSTALS AND DIRECTIONALLY SOLIDIFIED INGOTS OF TiAl-BASE ALLOYS

M. YAMAGUCHI

Department of Materials Science and Engineering, Kyoto University, Kyoto 606-8501, Japan

ABSTRACT

About a decade ago, a new approach for studying the lamellar microstructure of TiAl-base alloys was introduced by producing polysynthetically twinned (PST) crystals where the entire crystal consists of only a single lamellar grain. The deformation and fracture mechanisms and macroscopic flow behavior of the lamellar microstructure have all been extensively researched by the use of PST crystals. Results from these studies on PST crystals have shown that the optimum combination of strength, toughness and ductility can be obtained if the lamellar microstructure is aligned parallel to the test axis. One way to produce such an aligned lamellar microstructure is by directionally solidifying TiAl-based alloys. In this paper, first the results of the studies of the fundamental mechanical properties of PST crystals are summarised, and the results of our recent studies on the mechanical properties of directionally solidified ingots of TiAl-base alloys are then presented.

KEYWORDS

Intermetallic compounds, TiAl-base alloys, polysynthetically twinned (PST) crystals, directional solidification, deformation, fracture.

INTRODUCTION

TiAl-base alloys with two-phase structures consisting of the major γ (TiAl) and minor α_2 (Ti₃Al) phases have been much more intensively studied than other stable aluminides and their alloys in the Ti-Al system. There are two reasons. Firstly, their low density, strength and modulus retention at high temperatures, some tensile ductility at room temperature, and reasonably good oxidation resistance are very attractive as a new class of light-weight high-temperature materials for structural applications. Secondly, TiAl-base alloys can be processed almost similarly to metals and alloys through conventional manufacturing processes such as ingot melting, casting, forging, precision casting and machining on almost conventional equipment. In particular, it is essentially important that TiAl-base alloys are somewhat ductile even at room temperature and thus they are readily castable using standard titanium casting processes. Otherwise, the pace of the research and development of TiAl-base alloys for structural applications would have been slackened quickly.

Recently the development of TiAl-base alloys has reached the point where turbine rotor wheels of TiAl-base alloys have started to be used in turbochargers for commercial passenger cars [1]. Not only turbocharger rotor wheels but also various blades of TiAl-base alloys for turbine engines have been tested. There is little doubt that such progress in the development of TiAl components is caused by recent extensive progress and improvements made in the

science and technology of TiAl-base alloys. However, more improvements over their properties and significant reduction in production costs of TiAl components are still required for widespread use of these alloys.

Engineering TiAl-base alloys generally start solidification as the β phase and go through the α single-phase region and $\alpha \Rightarrow \alpha + \gamma$ and $\alpha + \gamma \Rightarrow \alpha_2 + \gamma$ reactions, producing a $(\gamma + \alpha_2)$ two-phase structure. Thus, some different two-phase structures can be obtained by manipulating these phase transformation reactions. Since the mechanical properties of TiAl-base alloys strongly depend on their microstructure, their mechanical properties can be tailored to meet the needs for a specific component by controlling their microstructure. This is of great merit for TiAl-base alloys and has aroused a great deal of fundamental research on microstructure/property relationships in TiAl-base alloys. Recently, much effort has gone into developing basic technologies to control their lamellar microstructure by directional solidification (DS) and investigating the creep behavior and strength of DS processed ingots. In this paper, some basic studies leading to the development of DS processing of TiAl-base alloys and the microstructure and mechanical properties of DS processed TiAl-base alloys will be reviewed.

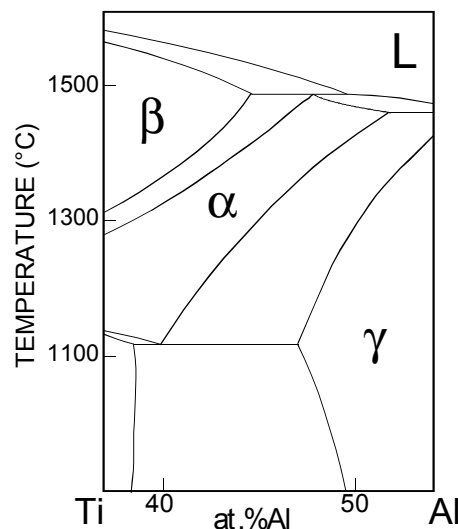


Fig. 1. Mid-section of the Ti-Al phase diagram. γ (TiAl), α_2 (Ti₃Al), α and β are intermetallics and solid solution phases with L1₀, D0₁₉, hcp and bcc structures, respectively.

MICROSTRUCTURE

When γ / α_2 two-phase alloys with nearly stoichiometric or Ti-rich compositions are prepared by usual melting-and-casting processes, a polycrystalline lamellar structure is formed. When these two-phase alloys with such a lamellar structure are heated or hot-worked at temperatures higher than 1150°C in the $(\alpha + \gamma)$ region, the lamellar structure is destroyed and a duplex structure consisting of equiaxed grains with the γ single-phase and the lamellar structure is formed. Microstructures of these two types exhibit very different mechanical properties. In general, fine and homogeneous duplex structures result in good ductility. The lamellar microstructures are poor in ductility; however, they are generally superior to the duplex structures in other mechanical properties such as fracture toughness, fatigue resistance and high-temperature creep strength.

γ and α_2 lamellae in the lamellar microstructures are stacked such that a $\{111\}_\gamma$ plane is parallel to $(0001)_{\alpha_2}$ and the closely packed directions on the $\{111\}_\gamma$ are parallel to those on $(0001)_{\alpha_2}$. However, the $[\bar{1}10]$ direction and the other two $[10\bar{1}]$ and $[0\bar{1}1]$ directions on (111) in the γ phase are not equivalent to each other because of the tetragonal $L1_0$ structure of the γ phase (Fig.2a) while directions of $\langle 11\bar{2}0 \rangle$ on the basal plane in the α phase (hcp) and α_2 phase (hexagonal $D0_{19}$) are all equivalent (Fig.2b). Thus, when the γ phase precipitates from the α parent phase, the $L1_0$ structure can be formed in six orientation variants corresponding to the six possible orientations of the $[\bar{1}10]$ direction along a reference $\langle 11\bar{2}0 \rangle$ direction of the α phase and thus of the α_2 phase [2].

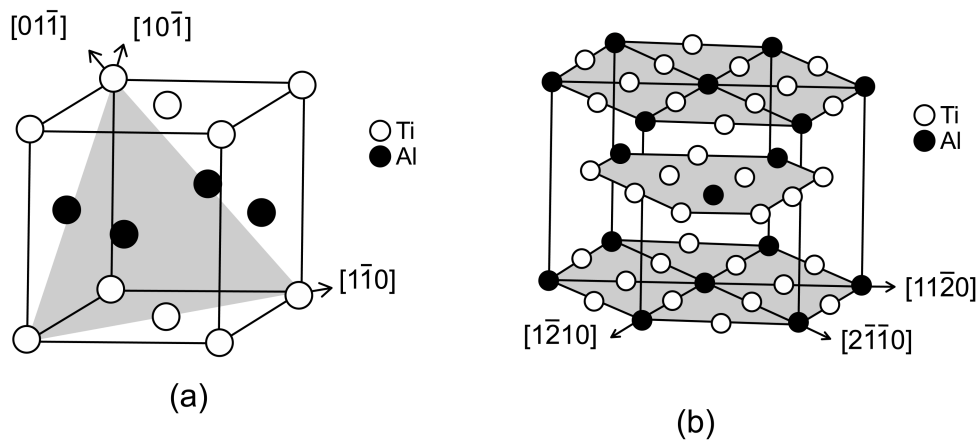


Fig.2. Crystal structures of the (a) $L1_0$ and (b) $D0_{19}$ types

When one γ plate impinges on another γ plate, one γ plate can be rotated by θ , which can be $60^\circ \times n$ ($n = 0 \sim 5$), and/or translated by \mathbf{f} , which can be 0 , $1/2\langle 10\bar{1} \rangle$, $1/6\langle 11\bar{2} \rangle$ and $1/6\langle 1\bar{2}1 \rangle$, with respect to the other γ plate (Fig. 3). The three non-zero \mathbf{f} vectors correspond to fault vectors for APB, SISF and CSF in the γ phase [3,4]. When $f = 0$, γ/γ lamellar boundaries resulting from such impingement of γ plates are of the true-twin type ($\theta = 180^\circ$), the 120° -rotational type ($\theta = 120^\circ, 240^\circ$) or the pseudo-twin type ($\theta = 60^\circ, 300^\circ$). Both positions and species of atoms are mirror images across the true-twinning plane while only atom positions are mirror images across the pseudo-twinning plane assuming that the c/a axial ratio of the γ phase is unity. γ/γ lamellar boundaries with an APB-type shift were observed in TiAl alloys [5,6]. However, the large majority of γ/γ lamellar boundaries are believed to be one of the three types with $f = 0$.

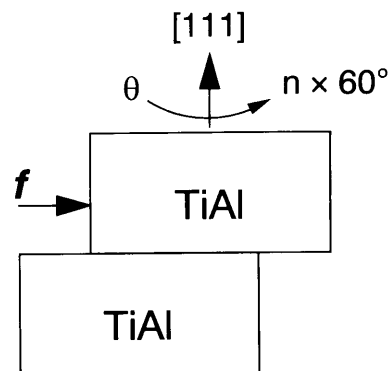


Fig. 3. Translational and rotational operations to create planar faults [3].

Domains of different variant types can coexist within each γ lamella [2]. Boundaries between such domains are simply termed domain boundaries [2]. Such domain boundaries as well as γ/γ lamellar boundaries are all γ/γ intervariant boundaries, although domain boundary planes do not show any preference for a specific crystallographic plane [2]. Atomic planes parallel to the lamellar boundaries in domains coexisting in a γ lamella stack in the same sequence, either abcabc.... or cbacba....[2], and thus two neighboring variants in a γ lamella are always of the 120° -rotational type with or without $\mathbf{f} \neq 0$. The reason for this has yet to be clarified. However, this is believed to be closely associated with the growth mechanism of γ lamellae in the parent α phase probably involving the motion of $1/3\langle 10\bar{1}0 \rangle$ type Shockley partial dislocations on alternate basal plane of the parent phase, similarly to the case of hcp-to-fcc structural change [7-9]. Of the three different types of lamellar boundaries, those of the true-twin type with the lowest energy are most frequently observed [10]. The growth process of γ lamellae must involve a mechanism to maximise the occurrence of true-twin type γ/γ lamellar boundaries [10,11]. Thus, the lamellar structure of two-phase TiAl-base alloys can be schematically described as in Fig. 4 [2].

MECHANICAL PROPERTIES OF LAMELLAR STRUCTURE

Mechanical properties of the lamellar microstructure of TiAl-base alloys depend on the relative orientation of the lamellar boundaries and loading axis and lamellar microstructural variables such as grain size, thickness and spacing of γ and α_2 lamellae and γ domain size. However, the lamellar orientation exerts a much greater influence on the mechanical properties of the lamellar structure than other lamellar microstructural variables. A new approach for studying mechanical properties of the lamellar microstructure of TiAl-base alloys was introduced in 1990 by producing crystals where the entire crystal consists of only a single lamellar grain [12]. Since numerous thin twin related lamellae are contained in the major constituent γ phase, these crystals were named polysynthetically twinned (PST) crystals from analogy with the phenomenon, “polysynthetic twinning” which is often observed in mineral crystals. PST crystals is in a sense a single crystal of the fully lamellar polycrystalline alloy. Since then, fundamental properties of the lamellar microstructure such as

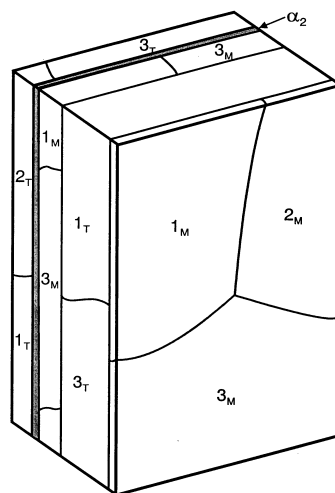


Fig. 4. Schematic illustration of the lamellar structure of TiAl-base alloys. 1_M - 3_M and 1_T - 3_T are matrix and twin variants [2].

microstructural characterization, deformation, fracture toughness and macroscopic flow behavior have all been extensively studied by the use of PST crystals.

What the studies using PST crystals have typically clarified is the effect of lamellar orientation on the mechanical properties and the anisotropic macroscopic flow behavior of the lamellar microstructure. The tensile properties of PST crystals depend strongly on the angle ϕ between the loading axis and lamellar boundaries. Figure 5 shows the ϕ dependence of the yield stress and tensile elongation of PST crystals of Ti-49.3Al (alloys compositions are given in at.%) at room temperature. PST crystals exhibit the highest strength at $\phi = 90^\circ$, however, tensile ductility at $\phi = 90^\circ$ is almost zero. A good balance of strength and ductility is obtained at $\phi = 0^\circ$, where strength is not as high as that for $\phi = 90^\circ$ but tensile ductility is as large as 5 - 20% at room temperature. When ϕ is in the range of $30^\circ - 60^\circ$, yield stress is much lower and elongation is much higher than $\phi = 0^\circ$ and $\phi = 90^\circ$ [2,13].

This trend remains unchanged almost up to 1000°C [14]. The ϕ dependence of the yield stress and tensile elongation of PST crystals is resulted from that shear occurs parallel to the lamellar boundaries (deformation in soft mode) for $\phi = 30^\circ - 60^\circ$ but it occurs mostly on $\{111\}$ planes intersecting the lamellar boundaries (deformation in hard mode) for $\phi = 0^\circ$ and $\phi = 90^\circ$. The large difference in yield stress between orientations for deformation in soft and hard modes can be mostly interpreted in terms of the Hall-Petch mechanism and the Schmid factors on the operative slip and /or twinning systems [15-17]. The mean free path of the dislocations in soft mode corresponds to the average size of domains in γ lamellae which is

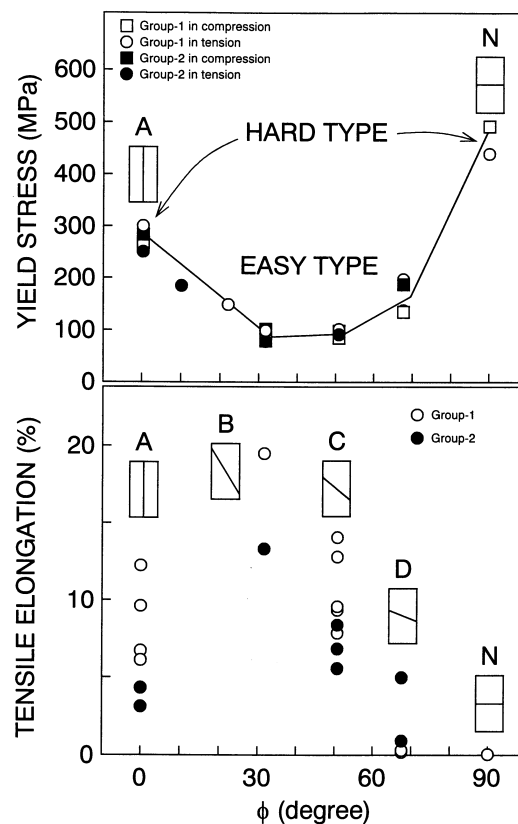


Fig. 5. The yield stress and tensile elongation of PST crystals at room temperature are plotted as a function of the angle ϕ between the loading axis and lamellar boundaries [13].

about two orders of magnitude greater than the average thickness of γ lamellae corresponding to the mean free path of the hard mode dislocations.

Ordinary slip on $\{111\}\langle 110\rangle$, superlattice slip on $\{111\}\langle 101\rangle$ and twinning on $\{111\}\langle 11\bar{2}\rangle$ can be operative in the γ phase in γ/α_2 two-phase alloys and the difference in the critical resolved shear stress between these systems is not significant [14]. In general, a combination of ordinary slip, superlattice slip and/or twinning systems operates in domains of each orientation variant. The combination of operative systems and the amount of shear produced by each slip or twinning system has been found to be determined so that deformation incompatibility at the lamellar and domain boundaries is minimized [18]. When $\phi = 0^\circ$, requirements for strain continuity at the domain and lamellar boundaries are almost satisfied [18]. This is a major reason for tensile ductility as large as 5 - 10% at room temperature for $\phi = 0^\circ$.

Fracture toughness of PST crystals is also sensitive to the relative orientation of the notch and lamellar boundaries. It is high when the notch orientation is of the crack-arrester or the crack-divider type and it is very low for the crack-delamination orientation [19]. The fatigue [20] and creep strength [21,22] of PST crystals depend on ϕ similarly to their yield strength. Thus, the best combination of the high-temperature strength, room-temperature ductility and fracture toughness is expected to be achieved through growing composite microstructures such as that of Fig.6 by directional solidification.

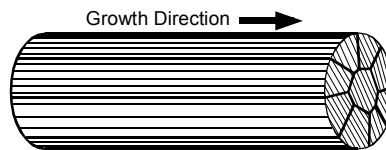


Fig. 6. DS ingot with one lamellar orientation.

LAMELLAR MICROSTRUCTURE CONTROL BY DIRECTIONAL SOLIDIFICATION

The main difficulty in microstructural control by directional solidification is that the lamellar microstructure is not formed from the liquid but from the solid state. The lamellar structure of TiAl-base alloys consists of lamellae of the γ and α_2 phases with the $(111)_\gamma // (0001)_{\alpha_2}$ orientation relationship. Hence, to control the lamellar microstructure, the orientation of the high temperature α phase must be controlled. However, the preferred growth direction of α dendrites is parallel to the $[0001]$ direction, and thus simple casting operations usually result in the lamellar microstructure with the lamellar boundaries perpendicular to the growth direction. When the β phase is formed during solidification, the resulting ingot is expected to have a microstructure consisting of columnar grains with the lamellar boundaries oriented parallel and 45° to the growth direction since the β phase grows along $\langle 100\rangle$ and the hcp α phase is formed from the bcc β phase following the Burgers orientation relationship. Thus, to achieve the fully lamellar microstructure with all the lamellar boundaries parallel to the growth direction by directional solidification, appropriate processing techniques have to be developed.

One way is by using a seed material [2,23-28]. To control the orientation of the α phase from the liquid, an appropriately oriented seed crystal can be used. The main problem with this approach is finding a suitable seed material. The seed materials must satisfy at least the following requirements.

(1) The high-temperature α phase formed in the seed must have the same orientation as that of the α_2 phase in the original lamellar microstructure. Thus, upon heating to just below the melting temperature, the lamellar microstructure must not be recrystallized and the volume fraction of the α phase must increase by the thickening of the α lamellae without losing its original orientation.

(2) In addition, the high-temperature α phase must be in contact with the liquid phase during directional solidification. Thus, the composition of the seed material must be in the range where the α phase is the primary phase to solidify or if primary β solidification occurs, an appropriate amount of the α phase solidifying in the interdendritic or intercellular regions of the β phase is ensured.

Suitable seed compositions were identified in TiAl-Si, TiAl-Mo-C and TiAl-Mo-Si systems. Ti-43Al-3Si and Ti-46Al-1.5Mo-1.0~1.5Si alloys are typical seed alloys used for our directional solidification experiments. The Ti-43Al-3Si alloy solidifies through the α phase while the other alloys do through the β phase. Our seed alloys normally contain some amounts of Si to promote α solidification or ensure an appropriate amount of the interdendritic α phase and to suppress recrystallization of the lamellar structure. The β solidification seed alloys are used to control the lamellar microstructure of alloys with compositions similar to the seed alloy. The Ti-43Al-3Si seed alloy can be used as a seed material for alloys with a wide variety of compositions, though it is brittle in comparison to the β solidification seed alloys of the TiAl-Mo-Si system since it contains very large Ti_5Si_3 particles formed from the liquid.

During the initial seeding, a portion of the seed is always melted first before the master ingot is allowed to come into contact with the liquid to complete the molten zone. This procedure is used to ensure that the composition of the initial molten zone is closer to that of the seed material. Since the Ti-43Al-3Si seed alloy is rich in Al and Si which are effective in increasing the stability of the α phase, the nucleation of the β phase can be prevented and the α phase can grow from the seed at the initial stage of seeding. Thus, the lamellar microstructure of TiAl-base alloys solidifying through not only the α phase but also the β phase can be controlled using the Ti-43Al-3Si seed alloy provided the solidification path of the master ingot is appropriate for the seeding approach.

The next problem is designing alloy composition so that the solidification path is suitable for the lamellar structure to be controlled using a seed crystal of the Ti-43Al-3Si seed alloy. Through seeding experiments of binary TiAl alloys, the orientation of the lamellar microstructure of Ti-47Al alloy was found to be controlled using the seed alloy. Similarly to the Ti-47Al alloy, seeding should be possible for multi-component alloys based on this alloy if alloying may not cause any significant change in the solidification path of the base alloy. Adding elements promoting the stability of the β phase (β stabilizers) shifts the primary β region towards the Al-rich side and adding α stabilizers such as Si and C shifts the primary α

region towards the Ti-rich side. Table 1 shows that how much shift of the α/β primary region boundary of the equilibrium liquidus surface in the Ti–Al system is caused by adding 1 at. % of each of the nine elements [28]. We call such a specific value of shift for each element “Al-equivalent” which is positive for β stabilizers and negative for α stabilizers.

When the alloying elements and the amount of each element to be added to the base Ti-47Al alloy are determined, the Al content of the base alloy is modified to let the relative position of the α/β primary region boundary remain as that is in the binary system. The Al content of the new alloy, c_{Al} can be calculated using the following equation [28].

$$c_{Al} = 47 + aX_{eq} + bY_{eq} + cZ_{eq} + \dots$$

where a , b , c and X_{eq} , Y_{eq} , Z_{eq} are the amount and the Al-equivalent of alloying elements X ,

Table 1. Al-equivalent values for typical alloying elements for TiAl-base alloys

C	Si	Cr	V	Nb	Ta	Mo	Re	W
-4.2	-2.8	+0.1	+0.3	+0.3	+0.3	+0.6	+0.8	+1.0

Y , Z , respectively. When approximately $46 < c_{Al} < 48$, the lamellar microstructure can be aligned along the growth direction using a seed of the Ti-43Al-3Si seed alloy at a growth rate of 10 mm/h. A well aligned lamellar microstructure can be produced for a wider range of c_{Al} for a slower growth rate.

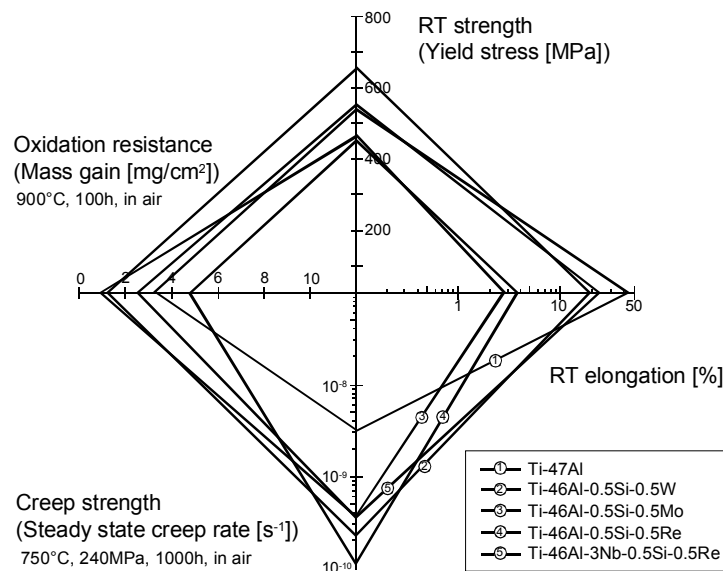


Fig. 7. Mechanical properties and oxidation resistance of DS ingots of some TiAl-base alloys [28].

MECHANICAL PROPERTIES OF DS INGOTS OF SOME TiAl-ALLOYS

A wide variety of TiAl-base alloys are directionally solidified using the Ti-43Al-3Si seed alloy and their mechanical and oxidation properties were examined. Figure 7 shows the

mechanical and oxidation properties of DS ingots of Ti-47Al, Ti-46Al-0.5Si-0.5Re, Ti-46Al-0.5Si-0.5W, Ti-46Al-0.5Si-0.5Mo and Ti-46Al-3Nb-0.5Si-0.5Re alloys in which the lamellar boundaries are aligned parallel to the growth direction at a growth rate of 10 mm/h [28]. The room-temperature yield stress and tensile elongation were obtained using small tensile specimens with a gauge length of $5 \times 2 \times 0.5 \text{ mm}^3$. The small specimen size may have enhanced tensile ductility. Even taking that into account, the DS ingots still exhibit an excellent combination of mechanical properties. In particular, their creep resistance is excellent [28,29]. Creep tests were performed in air at 750°C and 240MPa using specimens with a gauge size of 30 mm in length and 6 mm in diameter. Creep curves corresponding to the creep data in Fig.7 are shown in Fig. 8 [28]. It should be noted that not only the secondary creep rate but also primary creep strain is reduced by aligning the lamellar boundaries along the loading axis. The secondary creep rate of the binary Ti-47Al alloy under the creep condition is $2.07 \times 10^{-9} \text{ s}^{-1}$, which is still comparable to or lower than that reported for the highly alloyed advanced TiAl-base polycrystalline alloys [30,31], is much higher than those for the quaternary and quinary alloys. It is of interest to note that the addition of a small amount of Si and transition metals such as Mo, W and Re dramatically increases creep resistance of DS ingots of TiAl-base alloys [28].

CONCLUSIONS

1. The operative slip and/or twinning systems for each orientation variant of the γ phase in PST crystals are determined so that strain incompatibility at the domain and lamellar boundaries is minimized. When the lamellar boundaries are parallel to the loading axis,

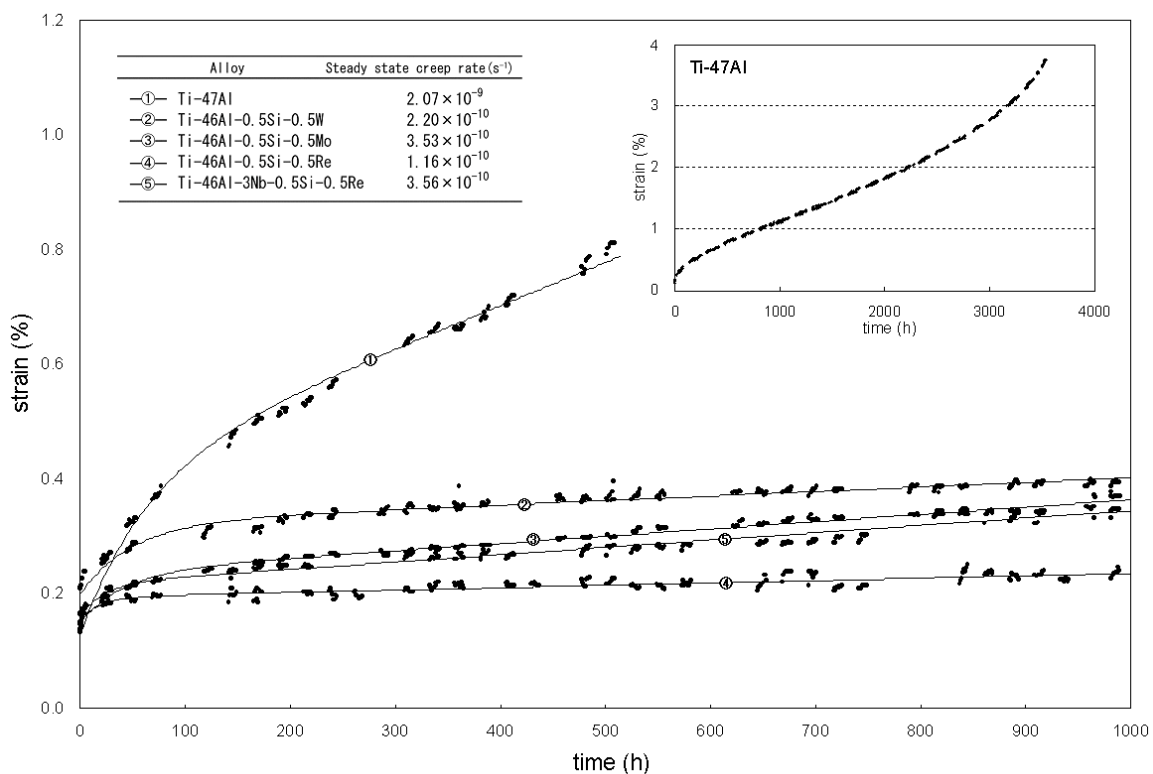


Fig. 8. Creep curves corresponding to the steady state creep rates of the five alloys given in Fig. 7 [28].

requirements for strain continuity at the domain and lamellar boundaries are almost satisfied, and thus a good combination of strength and ductility is obtained for this orientation. This discovery stimulated the research and development of directional solidification of TiAl-base alloys to produce a columnar grain material with the lamellar orientation aligned parallel to the growth direction.

2. A single-crystal (PST) like structure with each columnar grain having the same orientation can be grown by directional solidification techniques and a seed material.
3. The directionally solidified ingots with an aligned lamellar microstructure exhibit a good balance of room temperature tensile properties and creep strength.

REFERENCES

- [1] Tetsui T.: *Current Opinion in Solid State & Materials Science*, 4, (1999) 243.
- [2] Yamaguchi M., Inui H. and Ito K.: *Acta Mater.*, 48, (2000) 307.
- [3] Yoo M. H. and Yamaguchi M.: In: *Microstructure and Properties of materials*, J. C. M. Li (Ed.). World Scientific, Singapore, 2000, pp. 79-138.
- [4] Rao S. Woodward C. and Hazzledine P. M.: In: *Defect-Interfaces Interactions*, E. P. Kvam, A. H. King, M. J. Mills, T. D. Sands and V. Vitek (Eds.). MRS, Pittsburgh, PA, 1994, p. 285.
- [5] Denquin A. and Naka S.: *Phil. Mag. A*, 68, (1993) 13.
- [6] Ricolleau Ch., Denquin A. and Naka S.: *Phil. Mag. A*, 69, (1994) 197.
- [7] Yang Y. S. and Wu S. K.: *Phil. Mag. A*, 1992, 65, (1992) 15.
- [8] Singh S. R. and Howe J. M.: *Phil. Mag. A*, 1992, 66, (1992) 739.
- [9] Kad B. K., Hazzledine P. M. and Fraser H. L.: In: *Defect-Interfaces Interactions*, E. P. Kvam, A. H. King, M. J. Mills, T. D. Sands and V. Vitek (Ed.). MRS, Pittsburgh, PA, 1994, p. 311.
- [10] Zghal S., Naka S. and Couret A.: *Acta Mater.*, 45, (1997) 3005.
- [11] Oh M. H., Inui H., Nakamura A. and Yamaguchi M.: *Acta Metall. Mater.*, 40, (1992) 167.
- [12] Fujiwara T., Nakamura A., Hosomi M., Nishitani S. R., Shirai Y. and Yamaguchi M.: *Phil. Mag. A*, 61, (1990) 591.
- [13] Inui H., Oh M. H., Nakamura A. and Yamaguchi M.: *Acta Metall. Mater.*, 40, (1992) 3095.
- [14] Inui H., Kishida K., Misaki M., Kobayashi M., Shirai Y. and Yamaguchi M.: *Phil. Mag. A*, 72, (1995) 1609.
- [15] Hazzledine P. M., Kad B. K. and Mendiratta M. G.: *Thin film: Stresses and Mechanical Properties IV*, P. H. Townsend, T. P. Weihs, J. E. Sanchez and P. Borgesen (Eds.). MRS, Warrendale PA, 1993, p. 725.
- [16] Parthasarathy T. P., Mendiratta M. G. and Dimiduk D. M.: *Acta Mater.*, 46, (1998) 4005.
- [17] Kishida K., Johnson D. R., Masuda Y., Umeda H., Inui H. and Yamaguchi M.: *Intermetallics*, 6, (1998) 679.
- [18] Kishida K., Inui H. and Yamaguchi M.: *Phil. Mag. A*, 78, (1998) 1.
- [19] Yokoshima S. and Yamaguchi M.: *Acta Mater.*, 44, (1996) 873.
- [20] Nakano T., Yasuda H. Y., Higashitani N. and Umakoshi Y.: *Acta mater.*, 45, (1997) 4807.
- [21] Matso T., Nozaki T., Asai T., Chang S. Y. and Takeyama M.: *Intermetallics*, 1998, 6, (1998) 695.

- [22] Wegmann, G., Yamamoto, R., Maruyama, K., Inui, H. Yamaguchi, M.: *Gamma Titanium Aluminides 1999*, Y-W. Kim, D. M. Dimiduk, M. H. Loretto (Eds.). TMS, Warrendale, 1999, p. 717.
- [23] Yamaguchi M., Johnson D. R., Lee H. N. and Inui H.: *Intermetallics*, 8, (2000) 511.
- [24] Johnson D. R., Inui H. and Yamaguchi M.: *Acta Mater.*, 44, (1996) 2523.
- [25] Johnson D. R., Masuda H., Inui H. and Yamaguchi M.: *Acta Mater.*, 45, (1997) 2523.
- [26] Johnson D. R., Chihara K., Inui H. and Yamaguchi M.: *Acta Mater.*, 46, (1998) 6529.
- [27] Lee H. N., Johnson D. R., Inui H., Oh M. H., Wee D. M. and Yamaguchi M.: 48 (2000) 3221.
- [28] Muto S., Yamanaka T., Lee H. N., Johnson D. R., Inui H. and Yamaguchi M.: *Adv. Eng. Mater.*, 3 (6) (2001) in press.
- [29] Thomas M. and Naka S.: In: *Gamma Titanium Aluminides 1999*, Y-W. Kim, D. M. Dimiduk and M. H. Loretto (Eds.). TMS, Warrendale, PA 1999, p.633.
- [30] Kim Y-W. and Dimiduk D. M.: In: *Structural Intermetallics 1997*, M. V. Nathal, R. Darolia, C. T. Liu, P. L. Martin, D. B. Miracle, R. Wagner and M. Yamaguchi (Eds.). TMS, Warrendale, PA 1997, p.531.
- [31] F. Appel F. and R. Wagner R.: *Mater. Sci. Eng. R*, 22, (1998) 187.